Available online at www.sciencedirect.com
SCIENCE DIRECT
Journal of Photochemistry and Photobiology A: Chemistry 181 (2006) 370–377
Journal of Photochemistry and Photobiology A:Chemistry
www.elsevier.com/locate/jphotochem

Excited state acidity of bifunctional compounds 9. Excited state intramolecular proton transfer in 3,5-dihydroxy-7,4′-dimethoxyflavone and 3,5-dihydroxy-7,4′-dimethoxyflavanone: spectral and fluorescence decay results☆

Samira G.M. Portugal[a,1], Luis A. Montero-Cabrera[b], Lourdes A. Diaz[b], Ira M. Brinn[a,*]

[a] *Laboratório de Espectroscopia Resolvida no Tempo (LERT), Instituto de Química, Universidade Federal do Rio de Janeiro, C.P. 68.563, Ilha do Fundão, Rio de Janeiro, RJ 21.945-900, Brazil*
[b] *Universidad de La Habana, Facultad de Quimica, La Habana 10400, Cuba*

Received 31 May 2005; received in revised form 16 December 2005; accepted 19 December 2005
Available online 2 February 2006

Abstract

Both title compounds show two fluorescence bands, with maxima at approximately 290 nm and 340 nm in non-protic (hexane, cyclohexane) and protic (ethanol) solvents. Approximate molecular orbital calculations suggest that these two bands can be associated with an excitation partially localized on the anisolyl moiety and a more delocalized excitation, respectively, present in both compounds. In cyclohexane both compounds exhibit a fluorescence band with a maximum at 550 nm, which can be associated with the proton transferred species. In the case of the flavanone this band is very weak and attributed to Excited State Intramolecular Proton Transfer (ESIPT) of the proton at the 5-position. In the flavone the corresponding band is considerably more intense and the theoretical calculations point to the proton being transferred as originating from the 5-position also.

In cyclohexane the flavanone exhibits monoexponential decay under the band at 290 nm. In all other combinations solute/solvent/band studied here the fluorescence was found to follow a biexponential decay. In the case of the flavanone these results are interpreted as indicating that the localized anisolyl excitation is not coupled to the delocalized excitation, whereas the decay of the latter is coupled to ESIPT. The time-resolved results of the flavone are interpreted as indicating coupling between all three excited states observed.

Keywords: ESIPT; Flavanoids; TCSPC; Fluorescence spectra; Molecular orbital calculations

1. Introduction

Flavonoids are ubiquitous in both animals and plants, where nature uses them, principally, to absorb, transfer and degrade energy, usually via electron transfer [1,2]. This leads to their unique pharmaceutical properties as antioxidants. Apart from these properties, they also hold quite a bit of interest for photochemists; the first proton transfer (PT) laser described [3] used a flavonoid analog, 7-hydroxy-4-methyl-coumarin. ESIPT of the flavonoids themselves, especially 3-hydroxy-flavone (3HF), has been studied [4–20] extensively over the last few years by various research groups. These studies have found that 3HF and some substituted analogs do undergo [9,17] lasing, that the emission characteristics in hydrocarbon solvents are a function [6,7,10] of the presence of hydrogen-bonding impurities, that the rate constant for ESIPT (k_{PT}) in a free jet is reasonably large [10,18] ($6.5 \times 10^{11}\ s^{-1}$) in the S_1 state, apparently consistent with the fact that under these conditions only the tautomeric fluorescence was observed, because k_{PT} is some three orders of magnitude greater than the rate constant for fluorescence. However, it should be borne in mind that a large k_{PT} does not necessarily

☆ Presented, in part, at the Eighth Inter-American Photochemical Society Conference, Foz do Iguaçu, Brasil, 1996.

* Corresponding author. Tel.: +55 21 2562 7251.
E-mail address: irabrinn@iq.ufrj.br (I.M. Brinn).
[1] Present address: Departamento de Ciências Exatas, Universidade Gama Filho, Rio de Janeiro, RJ, Brazil.

1010-6030/$ – see front matter © 2005 Elsevier B.V. All rights reserved.
doi:10.1016/j.jphotochem.2005.12.022

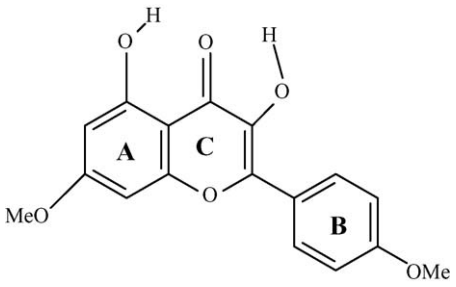

Fig. 1. Molecular structure of 3,5-dihydroxy-7,4′-dimethoxyflavone (DHF).

imply a high concentration of the PT species, because the reverse PT is even more rapid [11,16] ($1.7 \times 10^{13}\ s^{-1}$) in S_1. This process is slow [14–16] ($7 \times 10^{4}\ s^{-1}$) in the T_1 state, thus justifying the suggestion that lasing is due to ESIPT. For 3HF in methylcyclohexane (MCHx), two rise times in the appearance of the transient absorption spectrum of the PT species were determined [19] as 240 fs and 10 ps. These results were interpreted [19] as the 10 ps time being due to impurities in the MCHx and k_{PT} therefore being $4 \times 10^{12}\ s^{-1}$. By observing the effect of adding methanol to the cyclohexane (CHx) the same authors suggested that small quantities of methanol (MeOH) actually increased k_{PT} whereas an excess of MeOH inhibited ESIPT. The same conclusion was arrived at [11] from studies of 3HF on an Ar matrix at 10 K.

Investigation of ESIPT in other flavanoids is less common. A red shifted fluorescence band was observed [21] in an ethanol (EtOH) solution of 7-hydroxyflavone (7HF, which does not permit an intramolecular hydrogen bond). The interpretation given [21] was that this emission was due to the presence of a low concentration of the anion of 7HF. However, another study [22] of the fluorescence spectra of 7HF and 5-hydroxyflavone (5HF) showed that, in MCHx, the weak band attributed to the PT structure of 5HF (with maximum at 670 nm) is further red shifted than the corresponding band for 7HF (560 nm). These authors attributed both of these red bands to ESIPT.

We report below the spectroscopic and time resolved results of two flavanoids with hydroxyl groups in both the 3- and 5-positions, i.e., 3,5-dihydroxy-7,4′-dimethoxyflavone (DHF, Fig. 1) and 3,5-dihydroxy-7,4′-dimethoxyflavanone (DHAF, Fig. 2) the corresponding compound that has been reduced across the 2- and 3-positions. The main questions which are addressed here is to what extent the simultaneous presence of the 5-hydroxy group affects the photochemical behavior of the 3HF

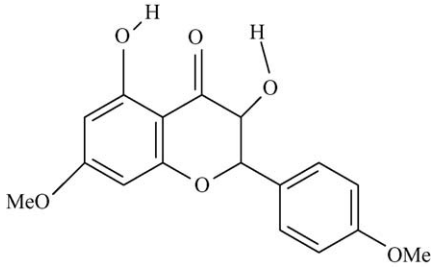

Fig. 2. Molecular structure of 3,5-dihydroxy-7,4′-dimethoxyflavanone (DHAF).

analog (DHF) and, in the presence of a non-aromatic 3-hydroxy group (DHAF) will the hydroxyl group in the 5-position undergo ESIPT.

Assuming that DHF undergoes ESIPT, two fluorescence bands would be expected, one attributable to the normal structure and one to the proton transferred structure. If DHAF then also showed two bands, the proton that was being transferred could only be from the 5-position and arguments based on the similarity of the two structures would indicate that DHF would also be transferring this same proton. If DHAF showed only one band, then the same arguments could be used to conclude that the ESIPT in DHF was due to the –OH group in the 3-position.

2. Methods

2.1. Experimental

DHF and DHAF were isolated [23] from the hexane extract taken from the trunk wood of *Aniba* sp. They were used without further purification, after verifying their purity with TLC, using dichloromethane (Merck, P.A.) as eluent. The molecular structures were verified by ^{1}H NMR in DMSO. The solvents used for spectroscopy were cyclohexane (CHx), *n*-hexane (Hx) and EtOH (all Merck, UVASOL). These were used without further purification. In the case of the time-resolved single photon counting experiments, the solutions were prepared immediately before the experiment, nitrogen was bubbled through the cell containing the sample for approximately 15 min and then the cell was maintained stoppered.

The Absorption spectra were taken on a Cary 1-E Spectrophotometer. The fluorescence spectra were obtained on a Hitachi F4500 Spectrophotofluorimeter, using Rhodamine B as an internal standard to correct the lamp output. The scattering signal from the lamp is then used to correct [24] the instrument response function, thus generating predominantly corrected spectra, although the tails of the lowest energy bands are outside of the correction region of the internal standard used. The time resolved measurements were done on the equivalent of an Edinburgh Analytical Instruments CD-900 Time Resolved Spectrometer, whose specifics have been given [25]. Emission is measured using a Hamamatsu R955 photomultiplier. The excitation lamp was typically used at a pressure of 300 mm Hg and pulsed at 40 kHz. Count rates did not exceed 1 kHz, to limit pileup errors. Because of the weakness of the fluorescence of the samples, the slits were maintained wide open (excitation slit = emission slit = 10 nm, iris of photomultiplier = 85) and counting was terminated when 1000 pulses were collected in the maximum channel.

2.2. Calculations

Molecular orbital calculations were done on the ground and first few electronically excited singlet states, using the CNDOL/22 version on the optimized structures shown in Figs. 1 and 2, in addition to the intramolecular proton transferred structures of each, considering the hydrogens from both hydroxyl groups in the case of DHF and only the hydroxyl group

in the 5-position in the case of DHAF. This version differs from the original [26] CNDOL method only to the extent that the diatomic electron repulsion integrals are calculated by means of a version of Ohno's [27] formula which was modified to conform to experimental values:

$$\gamma_{AB}^{lk} = (2(a_{AB}^{lk})^2 + a_{AB}^{lk} R_{AB} + 2(R_{AB}^2)^{-1/2}$$

$$a_{AB}^{lk} = 2(\gamma_{AA}^{ll} + \gamma_{BB}^{kk})^{-1}$$

The atomic coordinates used were the same for all of the electronic states of any given structure, i.e., those of the separately optimized ground states, even in the case of proton transferred structures. This was done using the PM3 semi-empirical Hamiltonian within the MOPAC6J version of the MOPAC v.6 program [28] developed in the Havana Laboratory.

Simulated fluorescence decay profiles were generated using a variation of a Monte Carlo method already described [29]. The previously used program was modified [30] to allow convolution of the fitted poly-exponential decay by a model lamp decay pulse. The latter was assumed to be a Gaussian with a fwha of 5 ns, a typical temporal width of the analytically more complicated lamp profile used in the equipment employed in these experiments. The reliability of the fitting procedure used here to analyze, as bi-exponentials, the experimental fluorescence decay profiles was evaluated by inputting the two fitted tau values and verifying if 1000 pulses in the maximum channel permitted recuperation of the original generating values. The input assumed that the contribution of the two terms was equal at time = 0, which is expected to be the optimum condition.

3. Results

3.1. Absorption spectra

The molar absorbtivities vs. wavelength of DHAF and DHF in CHx are shown in Fig. 3. DHAF shows a broad, weak first band with a maximum at approximately 340 nm and a slightly stronger second band with a maximum at 290 nm. For DHF the corresponding bands are considerably stronger, with maxima at approximately 370 nm and 330 nm.

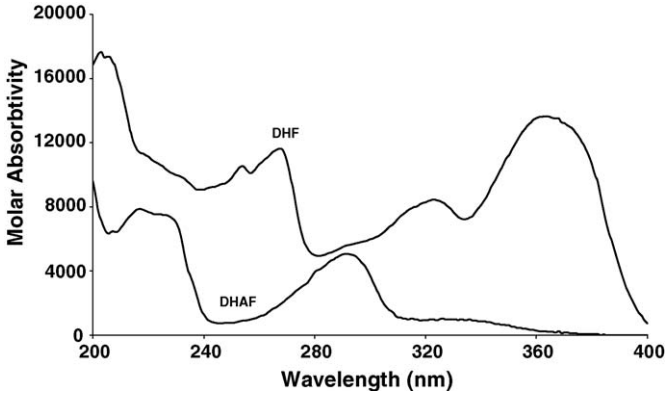

Fig. 3. Molar absorbtivity of DHF and DHAF in CHx.

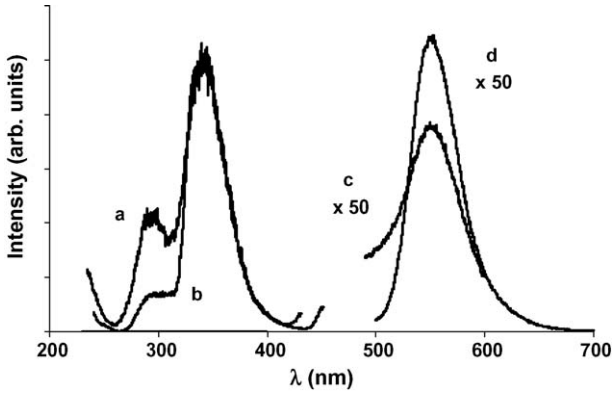

Fig. 4. Fluorescence spectra in CHx: (a) $\lambda_{EXC} = 225$ nm, [DHAF] = 5.21×10^{-6} M, (b) $\lambda_{EXC} = 230$ nm, [DHF] = 4.41×10^{-6} M, (c) $\lambda_{EXC} = 330$ nm, [DHAF] = 1.04×10^{-4} M and (d) $\lambda_{EXC} = 365$ nm, [DHF] = 4.41×10^{-5} M.

3.2. Fluorescence spectra

Sample fluorescence spectra of DHAF and DHF in CHx, at different excitation wavelengths, are shown in Fig. 4. In CHx both flavanoids exhibit a weak (and noisy) emission whose maximum is at approximately 290 nm, a stronger emission at 340 nm and a weak emission at 550 nm, extremely so in the case of DHAF. (This last band is shown with a magnification of 50.) In the case of the DHAF spectrum the separation of the 290 nm and 340 nm bands is considerably more obvious than in the case of the DHF spectrum.

3.3. Time-resolved results

A sample of the time-resolved single photon counting results is shown in Table 1. Although the calculated χ^2 values were all 1.0 ± 0.1, which would suggest that the fits have been optimized reasonably well, the simulations indicated that the calculated

Table 1
Fluorescence decay characteristic times (ns) of 3,5-dihydroxyflavanoids and anisole

λ_{EM} (nm)	CHx	EtOH
Anisole		
290[a]	6.79 ± 0.06	7.80 ± 0.03
DHAF		
290[a]	10.9 ± 0.1	7.59 ± 0.04
		19.42 ± 0.06
340[a]	1.38 ± 0.05	1.51 ± 0.03
	13.9 ± 0.3	6.1 ± 0.2
DHF		
290[a]	5.4 ± 0.6	6.6 ± 0.2
	19.3 ± 0.3	16.4 ± 0.8
340[a]	3.7 ± 0.1	5.9 ± 0.1
	22.2 ± 0.6	30.8 ± 0.6
550[b]	1.91 ± 0.03	–
	14.0 ± 0.7	

Errors given as one standard deviation.
[a] $\lambda_{EXC} = 270$ nm.
[b] $\lambda_{EXC} = 320$ nm.

tau values less than 5 ns are not reliable, consistent with the preliminary finding [30] that convolution of a poly-exponential decay by a lamp pulse which is temporally wider than any of the tau values is only reliable when the number of photomultiplier pulses collected is significantly greater (by one or more orders of magnitude) than that normally reported. In the trivial cases of anisole in CHx and EtOH shown in Table 1, a mono-exponential decay was obtained, as expected. In the case of DHAF in CHx, the decay profile taken at 290 nm a mono-exponential decay describes the data well, whereas a bi-exponential is required to fit the decay profile below the band at 290 nm in EtOH and the bands at 340 nm in both solvents. The fluorescence intensity at 550 nm was too weak in either solvent to permit a TRSPC determination. All of the fluorescence decay profiles of DHF in CHx and EtOH could be described adequately as bi-exponentials. For DHF in EtOH, the fluorescence intensity at 550 nm was too weak to allow a determination of the decay profile.

3.4. Molecular orbital calculations for optimized geometries

The PM3 Hamiltonian used to calculate the atomic coordinates for the ground and all electronically excited states, point out two important differences between DHAF and DHF. The first difference in the atomic coordinates of the two structures, as might be expected because of the presence of the tetrahedral carbon atom at position-2 of the former, involves the co-planarity of the conjugated systems. In the case of DHF, the nuclei of all of the heavy atoms are calculated to fit into a planar space 0.6 Å thick, whereas the corresponding plane for the DHAF structure is thicker than 3.0 Å. The second involves the position of the hydrogen atoms in the two hydroxyl groups. In both structures the calculated O–H distance at position-3 is 0.95 Å as compared to 0.96 Å at position-5. The H-bonding distance to the oxygen of the carbonyl group at position-4 varies with structure, in DHF being $r(C{=}O\cdots H_3) = 2.36$ Å, as compared to $r(C{=}O\cdots H_3) = 2.92$ Å in DHAF. However, surprisingly, $r(C{=}O\cdots H_5) = 1.82$ Å for both structures, suggesting that the H-bond to H_5 is stronger than that to H_3, even in DHF.

3.5. Molecular orbital calculations for excited states

Table 2 shows the lowest energy calculated vertical transitions (in nm) for the two flavanoids in the normal and proton transferred structures. The calculated oscillator strengths are given as a rough guide to the maximum fluorescence intensity expected. The values of the properties of those calculated states

Table 2
Theoretically calculated CNDOL properties of excited singlet states of 3,5-dihydroxyflavanoids

Flavanoid	λ (nm)	f[a]	$\Sigma\Delta\rho$[b]			$\Sigma\lvert\Delta\rho\rvert$[c]		
			A	B	C	A	B	C
DHF	466	0.00014	−0.20	+0.08	+0.16	0.20	0.21	0.38
	376	0.00054	−0.04	−0.06	−0.04	0.19	0.21	0.28
	356	0.0005	+0.26	−0.02	−0.18	0.44	0.04	0.20
	351	*0.13*	*−0.24*	*+0.16*	*+0.03*	*0.24*	*0.16*	*0.22*
	338	0.00004	−0.11	−0.01	+0.12	0.12	0.24	0.34
	296	*0.22*	*+0.03*	*−0.02*	*+0.04*	*0.13*	*0.10*	*0.28*
DHF (5-PT)	*497*	*0.00044*	*+0.01*	*+0.03*	*−0.01*	*0.16*	*0.07*	*0.26*
	388	0.00003	+0.09	−0.02	−0.11	0.26	0.08	0.55
	384	0.0025	0	−0.08	+0.06	0.12	0.14	0.19
	369	0.00069	+0.11	−0.08	+0.05	0.13	0.13	0.20
DHF (3-PT)	*609*	*<10^{-5}*	*−0.23*	*+0.11*	*+0.10*	*0.23*	*0.11*	*0.39*
	436	<10^{-5}	−0.06	0	−0.16	0.23	0.20	0.35
	424	0.087	−0.16	+0.06	+0.05	0.16	0.06	0.37
	405	<10^{-5}	−0.06	−0.05	+0.12	0.06	0.12	0.22
DHAF	359	0.0091	+0.11	+0.08	−0.14	0.32	0.09	0.14
	351	*0.15*	*−0.17*	*+0.13*	*+0.02*	*0.17*	*0.13*	*0.14*
	332	0.019	−0.05	+0.12	−0.08	0.24	0.12	0.21
	324	0.12	+0.06	+0.08	−0.13	0.25	0.08	0.18
	291	*0.020*	*−0.05*	*+0.11*	*−0.06*	*0.17*	*0.11*	*0.14*
	273	0.090	0	+0.04	−0.09	0.24	0.11	0.13
DHAF (5-PT)	*386*	*0.00068*	*+0.08*	*+0.06*	*−0.16*	*0.38*	*0.06*	*0.21*
	365	0.031	+0.01	+0.03	−0.05	0.12	0.08	0.09
	333	0.19	+0.18	+0.01	−0.19	0.38	0.05	0.20
	303	0.091	+0.14	−0.01	−0.16	0.41	0.06	0.22

The calculated properties of the two excited states of the normal structure (associated with the fluorescence bands observed at 290 nm and 350 nm) and the excited state of the PT structure (associated with the fluorescence bands observed at 550 nm) are shown in italics.

[a] Oscillator strength.

[b] Calculated sum of the charge density alterations upon excitation on the atoms of the three ring systems.

[c] Calculated sum of the absolute charge density alterations upon excitation on the atoms of the three ring systems.

Table 3
Calculated CNDOL oxygen charges on state attributed to S_1

Position (ring)	Charge density of electrons				
	DHF	DHF-3PT	DHF-5PT	DHAF	DHAF-5PT
3 (C)	−0.78	−0.86[a]	−0.79	−0.80	−0.82
4 (C)	−0.85[a]	−0.78	−0.80	−0.85[a]	−0.80
5 (A)	−0.77	−0.77	−0.85[a]	−0.77	−0.83[a]

[a] Carbonyl oxygen.

associated here with the observed fluorescence bands are given in italics.

The sum of the calculated electron density changes on the heavy atoms of each of the three rings, as well as the sum of their absolute values, during the transition from the ground state to each of the first few excited states, are shown in the last six columns of Table 2. It can be argued that these values can be used to characterize transitions as either being localized on a particular ring of the molecule or else delocalized over more than one ring. In principle, those transitions with small electron density changes on all three rings are interpreted as not involving electron redistribution between rings. In these cases, if any of the rings demonstrate a large value in the absolute electron density change, this is interpreted as indicating a transition which is localized on that particular ring.

Table 3 shows the calculated electron charges, in the excited state attributed to S_1, on the three oxygen atoms located at positions 3–5, i.e., those potentially involved in ESIPT. In all cases the calculated negative charge on the carbonyl oxygen is greater than that on either of the hydroxyl oxygens, however this difference is never greater than 10%.

4. Discussion

Considering the spectroscopy, one can see in Table 2 that the calculations predict that the Normal structures of both DHF and DHAF will have observable fluorescence bands (reasonable oscillator strengths) in the same region, at around 340–350 nm. Although the theoretically calculated energies do overstate the gap of the ESIPT band, they do correctly predict a red shift, compared to the spectrum of the Normal structure, via conversion of the lowest energy excited state from one which is not accessible via a one photon transition to one which is accessible, albeit through an extremely weak transition. It is difficult to compare experimental fluorescence intensities with theoretically calculated transition probabilities which do not take into account non-radiative pathways. Thus, the fact that the band attributed to the ESIPT structure of DHF is considerably more intense than the corresponding band of DHAF, despite the fact that that the theoretical calculations indicate that the latter has a slightly greater oscillator strength, can be rationalized by the latter having a greater non-radiative decay rate, and/or because of the approximate nature of our theoretical calculations. This might have been expected due to the more flexible molecular framework and the extra C–H vibrational frequencies, both of which can act as energy sinks, in the case of DHAF. In general, it can be considered that the observed behavior is consistent with the theoretically calculated results, with the above-cited exception of the calculations not localizing the PT band at 550 nm. Considering the calculated transition energies and electron density differences, as well as the fact that the fluorescence spectra of both flavanoids exhibit three bands whose maxima appear at approximately the same wavelengths, it seems reasonable to attribute the bands of the two flavonoids in a similar fashion.

The band with a maximum at 290 nm also is attributed to emission from the Normal structures and specifically from a mixture of excitations more localized on the individual rings (A–C rings in Fig. 1) in comparison with the band whose maximum appears at 340 nm, that is also attributed to emission from the Normal structure, however in this case the excitation is more delocalized. The observation of a second fluorescence band at 290 nm deserves further comment. The presence of two fluorescence bands attributed to the same species, although contradicting Kasha's Rule [31] and not very common, has been observed before. The observation in solution of simultaneous emission, $S_1 \rightarrow S_0$ and $S_2 \rightarrow S_0$, for toluene, benzene and p-xylene and $S_1 \rightarrow S_0$ and $S_3 \rightarrow S_0$, for naphthalene and pyrene [32] was reported several years ago. In addition, the observation of two bands in the fluorescence spectra of various derivatives of *p*-cyano-aniline has been amply reported [33–38], albeit the red-shifted band has been attributed usually to a second, radically altered ("twisted intramolecular charge transfer") structure. One might indicate that an alternative interpretation for the above-cited (TICT) spectra is that the emission is from two different excited states. Although this is, to the best of our knowledge, the first report of a band at 290 nm in flavones, there is precedence in the literature for the interpretation given here.

The band whose maximum appears at 550 nm is attributed to a proton-transferred (PT) form. In the case of DHAF, the proton being transferred is that in the 5-position, because only this hydroxyl group is connected to the conjugated system. The possibility of electronic excitation causing an increase in the acidity of the proton in the 3-position is simply ignored. In the case of DHF, in principle the proton being transferred could be from either the 3- or the 5-position. However, there are several factors which support the contention that what is being observed here is transfer of the proton in the 5-position. These are the following:

(1) The calculated oscillator strength for the long wavelength band is more than an order of magnitude greater in the case of the transfer being from the 5-position. This is also consistent with the experimental fact that the band at 550 nm is easily observable, albeit a weak transition.
(2) The total electronic energy is calculated to be some 9 eV lower for the case of transfer from the 5-position, as compared to transfer from the 3-position.
(3) Both –O–H···O=C distances in the ground state of DHF are considered to be within the bounds of pre-established H-bonds [39], however this distance is calculated to be 0.54 Å shorter in the case of the proton in the 5-position, which is considered to favor ESIPT via this proton. The hydrogen bond being shorter in the case of the hydroxyl group in the 5-position has been reported [40] for quercetin

(3,5,7,3′,4′-pentahydroxyflavone), based on both molecular orbital calculations and X-ray data. However, in the latter paper the interpretation given was, contrary to that given here, that the 5-hydroxyl group activated ESIPT of the 3-hydroxyl group. (The calculations done in this work actually show that the presence of the 5-hydroxyl group in DHF causes the hydrogen from the 3-hydroxyl group to move 0.04 Å further from the carbonyl oxygen, in comparison to 3HF.)

(4) The experimental fact that ESIPT is observed in DHAF is considered strong evidence for the existence of 5-hydroxyl ESIPT. The similarities between the spectra of DHAF and DHF are considered evidence for the same route being followed in the latter compound.

An interesting question which has been raised periodically is whether a better electronic description of the ESIPT structure is a covalent or a zwitterionic one. If it were strictly the former, the formal charges on the protonated and non-protonated oxygens would be equal. If the latter, the non-protonated oxygen would have approximately two more units of negative charge, compared to the protonated oxygen. Table 3 shows the theoretically calculated charge densities on the three oxygen atoms potentially involved in the ESIPT process and indicates that a covalent description is far superior to a zwitterionic description. Even taking into account the fact that molecular orbital calculations tend to exaggerate delocalization of electrons, the slight difference in calculated charges would appear to be too small to attribute integrally to a structural error in the calculational method chosen. This conclusion is consistent with the fact that no solvatochromic effect was detected in the ESIPT spectra observed here.

It is worth noting that an experimental answer to this question is extremely difficult to obtain, requiring determination and interpretation of the vibrational fine structure of an electronically excited state of a reasonably large molecule. To the best of our knowledge, this has been reported [41,42] only twice in the literature, where the resonance Raman spectra of *N*-(2-hydroxybenzylidene)aniline and 2-(2′-hydroxyphenyl)bezoxazole were taken and interpreted as favoring the zwitterionic structure, in the former case and the covalent structure in the latter case. Indirect evidence, that no correlation was found between non-radiative decay rates and solvent polarity for the ESIPT structure of 4-methyl-2,6-diformylphenol, was interpreted [43] as indicating that this species is better represented by a covalent structure.

The simplest possible description of this system is given by the kinetic Eqs. (1)–(5):

$$L^* \rightarrow G, \quad k_L \tag{1}$$

$$L^* \rightarrow D^*, \quad k_1 \tag{2}$$

$$D^* \rightarrow G, \quad k_D \tag{3}$$

$$D^* \rightarrow PT^*, \quad k_2 \tag{4}$$

$$PT^* \rightarrow PT, \quad k_{PT} \tag{5}$$

where L^* represents an electronic excitation which is localized on one ring, D^* an electronic excitation which is delocalized over the conjugated system, G the electronic ground state and PT represents the proton-transferred species. The system of coupled linear differential equations which describes this system is:

$$\frac{d[L^*]}{dt} = -(k_L + k_1)[L^*] \tag{6}$$

$$\frac{d[D^*]}{dt} = k_1[L^*] - (k_D + k_2)[D^*] \tag{7}$$

$$\frac{d[PT^*]}{dt} = k_2[D^*] - k_{PT}[PT^*] \tag{8}$$

Solving the above equations generates:

$$[L^*] = \alpha \exp\{-(k_L + k_1)t\} \tag{9}$$

$$[D^*] = \beta \exp\{-(k_L + k_1)t\} + \gamma \exp\{-(k_D + k_2)t\} \tag{10}$$

$$[PT^*] = \delta \exp\{-(k_L + k_1)t\} + \varepsilon \exp\{-(k_D + k_2)t\} + \zeta \exp\{-k_{PT}t\} \tag{11}$$

Before considering the time-resolved results of Table 1 and conciliating them with Eqs. (9)–(11), it is worthwhile reviewing some general considerations regarding fluorescence decay profiles. Neglecting contributions from impurities, poly-exponential decays from a single solute can be attributed to the presence of two or more electronically excited species whose kinetics are coupled via a rate constant that is approximately the order of magnitude of the decay constants for these species. The number of exponential terms should be equal to the number of species so coupled. However, it may not be possible to observe experimentally all of the terms present. Three different conditions could cause this: (a) one, or more, pre-exponential terms being considerably smaller than the others, therefore making a negligible contribution to the profile, (b) one, or more, exponential terms being considerably smaller or considerably larger than the others, therefore going off the scale of the instrument being used and (c) two, or more, exponential terms of approximately the same values, therefore difficult to separate by the data analysis program. In the case of the Time Correlated Single Photon Counting method, the fewer the pulses collected [29] the more likely the latter problem can occur. In addition, as the number of exponential terms increases, the probability of one of the above conditions holding also increases. Both the pre-exponential and exponential terms are functions of the various rate constants within the kinetic scheme which couples these species. Thus, the key to calculating the maximum number of exponential terms which potentially could be observed below any fluorescence band is knowing the number of distinct species present and the relative values of the rate constants which couple these. Unfortunately, in general, the rate constants are not known.

The fact that the fluorescence band at approximately 550 nm was not observed for either flavanoid dissolved in EtOH was interpreted as indicating that the OH groups of the solvent interact with the OH group at the 5-position of the flavanoids, inhibiting ESIPT. This observation is consistent with the observed

[19,44] complicated kinetics for flavanoids in alcohols, as well as the 10-fold decrease in fluorescence quantum yield observed [45] for 3HF in various alcohol solvents, relative to hexane.

If we consider the trivial cases of anisole in CHx and EtOH in Table 1, it is to be expected that only one species would be present, therefore the mono-exponential decay actually observed is reasonable. Considering the results of DHAF in CHx, the decay profile taken at 290 nm is again a mono-exponential, consistent with Eq. (9) and with the intuitive result that the anisolyl moiety, being out of the plane of the A and C rings, is not chemically coupled by any reaction which might be taking place on the nanosecond time scale. The bi-exponential decay encountered at 290 nm for DHAF in EtOH is in apparent contradiction with the model, however even in the case of the simpler 3HF system in alcohol solvents the process of ESIPT has proven [19,44,45] to be more complicated than expected. A possible explanation is that flavanols undergo photochemical oxidation, transferring an electron to either the EtOH and/or traces of water present, as has been observed [46] in indole and 7-azaindole, this reaction occuring on the same time scale as decay of the excited singlet. Considering the results of DHAF under the 340 nm band, a bi-exponential decay apparently was observed in both solvents, which would be consistent with Eq. (10). However the two tau values of approximately 1.5 ns are considered to be so suspect (in spite of the small errors attributed by the commercial fitting program) that it would be unwise to base a physical interpretation on these results.

Turning to the time-resolved results of DHF in Table 1, a bi-exponential decay is observed under the band at 290 nm in both solvents, in obvious contradiction of Eq. (9). The interpretation proffered here is that in DHF there is coupling between the B^* and AC^* states, due to the greater coplanarity of the rings, which is not possible in DHAF. The spectra in Figs. 4 and 5 offer some experimental support for this model, to the extent that there is greater overlap between the 290 nm and 340 nm bands in DHF, compared to DHAF. This can be factored into the kinetic model by altering step (2) to read:

$$L^* \Leftrightarrow D^*, \quad \frac{k_{1a}}{k_{1b}} \tag{2'}$$

which converts Eq. (9) into a bi-exponential. As predicted in Eq. (10) and observed in Table 1, bi-exponential decay is observed under the band at 340 nm. Finally, the time-resolved results of DHF in CHx under the band at 550 nm indicate a bi-exponential decay, whereas Eq. (11) predicts that a tri-exponential decay was to be expected. This can be rationalized as an erroneous fitting of the data, due to any of the three possible explanations indicated above; preference being given to the fact that only 1000 pulses could be collected in the maximum channel contributing heavily to this problem.

It is interesting here to point out that among the three states represented above, only two different molecular structures (normal and PT) are depicted. Thus this model can be considered to represent competitive kinetics [47] between charge transfer and proton transfer in the excited state. All three states are attainable within the duration of S_1 because both electron redistribution and ESIPT can occur on the same time scale as S_1 decay.

It is worth pointing out some differences between the observations recorded here and what has been reported for similar flavonoids. To the best of our knowledge, this is the first reported observation of the band at 290 nm. The 340 nm band assigned to D^* has been observed [4,6,7,44,48] in other flavanoids emitting in the 420–500 nm region. (It is common not to observe this band, when PT is considerably faster than decay.) The justification for the observation of this band at some 100 nm lower than previously reported may possibly be that the anisolyl moiety is folded out of the plane of the alkaloid moiety and thus the aromatic system is smaller than it would be if the rings were coplanar, however the presence of the hydroxyl group at position-5 would appear to be important. The band normally observed at wavelengths above 600 nm and attributed [4,6,7,44,48] to the tautomeric structure, is also observed here at a shorter wavelength, possibly for the same reason(s). The fact that the band at 550 nm is much stronger in the case of DHF, relative to DHAF, suggests that the non-radiative quantum yield is greater for the latter.

5. Conclusions

The steady-state fluorescence spectra of two similar flavanoides, DHF and DHAF, show three different bands. Results from time-resolved fluorescence decay profiles and approximate molecular orbital calculations have been combined to allow an interpretation of these surprising spectra. It is proposed that the three bands are due to; (1) a partially localized excited state on the anisolyl moiety, (2) the normal, more delocalized emission originating from rings "A" and "C" and (3) an ESIPT structure in which the proton transferred originally was on the hydroxyl group at position-5.

Acknowledgements

The authors gratefully acknowledge Prof. Raymond Zelnik (Universidade de São Paulo) who kindly donated the flavanoids used in this study, the Brazilian National Research Council (CNPq) for partial financial support (to S.G.M.P. and I.M.B.), the World Bank and the Fund for Studies and Projects (FINEP) for an equipment grant and the José Bonifácio University Foundation (FUJB), the Rio de Janeiro State Foundation for Research Support (FAPERJ) for maintenance grants, the Universidad Autónoma de Madrid for kindly providing the opportunity (to L.A.M.C.) for expanding the NDOL program in 2005, and the Council of State of the Republic of Cuba (Havana) and the Deutsche Akademischer Austauschdienst (Bonn, Germany) for equipment grants.

References

[1] V.A. Belyakov, V.A. Roginsky, W. Bors, J. Chem. Soc. Perkin Trans. 2 (1995) 2319–2326 (and references therein).
[2] T. Chan, G. Galati, P.J. O'Brien, Chem. Biol. Interact. 122 (1999) 15–25 (and references therein).
[3] A.M. Trozzolo, A. Dienes, C.V. Shank, J. Am. Chem. Soc. 96 (1974) 4699–4700.
[4] K. Sengupta, M. Kasha, Chem. Phys. Lett. 68 (1979) 382–385.

[5] A.J.G. Strandjord, S.H. Courtney, D.M. Friedrich, P.F. Barbara, J. Phys. Chem. 87 (1983) 1125–1133.
[6] D. McMorrow, M. Kasha, J. Phys. Chem. 88 (1984) 2235–2243.
[7] A.J.G. Strandjord, P.F. Barbara, J. Phys. Chem. 89 (1985) 2355–2361.
[8] T.P. Dzugan, J. Scmidt, T.J. Aartsma, Chem. Phys. Lett. 127 (1986) 336–342.
[9] P.-T. Chou, T.J. Aartsma, J. Phys. Chem. 90 (1986) 721–723.
[10] B. Dick, N.P. Ernsting, J. Phys. Chem. 91 (1987) 4261–4265.
[11] G.A. Brucker, D.F. Kelley, J. Phys. Chem. 91 (1987) 2856–2861.
[12] A. Mordzinski, Chem. Phys. Lett. 150 (1988) 254–258.
[13] G.A. Brucker, D.F. Kelley, J. Phys. Chem. 93 (1989) 5179–5183.
[14] W.E. Brewer, S.L. Studer, M. Standiford, P.-T. Chou, J. Phys. Chem. 93 (1989) 6088–6094.
[15] B. Dick, J. Phys. Chem. 94 (1990) 5752–5756.
[16] M.L. Martinez, S.L. Studer, P.-T. Chou, J. Am. Chem. Soc. 112 (1990) 2427–2429.
[17] D.A. Parthenopoulos, D. McMorrow, M. Kasha, J. Phys. Chem. 95 (1991) 2668–2674.
[18] A. Ito, Y. Fujiwara, M. Itoh, J. Chem. Phys. 96 (1992) 7474–7482.
[19] B.J. Schwartz, L.A. Peteanu, C.B. Harris, J. Phys. Chem. 96 (1992) 3591–3598.
[20] S.M. Ormson, R.G. Brown, F. Vollmer, W. Rettig, J. Photochem. Photobiol. 81A (1994) 65–72.
[21] M. Sarkar, P.K. Sengupta, J. Photochem. Photobiol. 48A (1989) 175–183.
[22] M.L. Martinez, S.L. Studer, P.-T. Chou, J. Am. Chem. Soc. 113 (1991) 5881–5883.
[23] H. Erdtman, L. Novotny, M. Romanuk, Tetrahedron (Suppl. 8) (1966) 71–74.
[24] W.H. Melhuish, J. Opt. Soc. Am. 52 (1962) 1256–1258.
[25] C.E.M. Carvalho, I.M. Brinn, A.V. Pinto, M.C.F.R. Pinto, J. Photochem. Photobiol. 123A (1999) 61–65.
[26] L.A. Montero, L. Alfonso, J.R. Alvarez, E. Pérez, Int. J. Quantum Chem. 37 (1990) 465–483.
[27] K. Ohno, Theor. Chim. Acta 2 (1964) 219–227.
[28] MOPAC6J, Semi-empirical Molecular Orbital Hamiltonians (MINDO/3, MNDO, AM1, PM3, MNDO/PDDG and PM3/PDDG) for Personal Computers, Havana, 1994-2004. Freely available from http://karin.fq.uh.cu/mopac6j-set.zip.
[29] L.T. Okano, A.C. Tedesco, A.T. Touso, D.R. Oliveira, M. Maeder, I.M. Brinn, J. Photochem. Photobiol. 175A (2005) 221–225.
[30] L.T. Okano, A.C. Tedesco, A.T. Touso, D.R. Oliveira, M. Maeder, I.M. Brinn, in preparation.
[31] M. Kasha, Disc. Far. Soc. 9 (1950) 14–19.
[32] F. Hirayama, T.A. Gregory, S. Lipsky, J. Chem. Phys. 58 (1973) 4696–4697.
[33] M. Kupfer, W. Abraham, Chem. Phys. Lett. 122 (1985) 300–302.
[34] D. Gormin, M. Kasha, Chem. Phys. Lett. 153 (1988) 574–576.
[35] A. Nag, T. Kundu, K. Bhattacharyya, Chem. Phys. Lett. 160 (1989) 257–260.
[36] R.K. Guo, N. Kitamura, S. Tazuke, J. Phys. Chem. 94 (1990) 1404–1408.
[37] K. Rotkiewicz, W. Rettig, J. Lumin. 54 (1992) 221–229.
[38] K. Hara, W. Rettig, J. Phys. Chem. 96 (1992) 8307–8309.
[39] A.L. Spek, J. Appl. Cryst. 36 (2003) 3–17.
[40] E. Falkovskaia, P.K. Sengupta, M. Kasha, Chem. Phys. Lett. 297 (1998) 109–114.
[41] W. Turbeville, P.K. Dutta, J. Phys. Chem. 94 (1990) 4060–4066.
[42] V. Kozich, J. Dreyer, A. Vodchits, W. Werncke, Chem. Phys. Lett. 415 (2005) 121–125.
[43] R. Das, S. Mitra, S. Mukherjee, Spectrochim. Acta 51A (1995) 363–369.
[44] J. Guharay, P.K. Sengupta, Spectrochim. Acta 53A (1997) 905–912.
[45] K.-J. Choi, B.P. Boczer, M.R. Topp, Springer Ser. Chem. Phys 38 (1984) 368–370.
[46] F. Gai, R.L. Rich, J.W. Petrich, J. Am. Chem. Soc. 116 (1994) 735–746.
[47] A. Douhal, M. Sanz, M.A. Carranza, J.A. Organero, L. Santos, Chem. Phys. Lett. 394 (2004) 54–60.
[48] P.-T. Chou, M.L. Martinez, J.H. Clements, J. Phys. Chem. 97 (1993) 2618–2622.